VNU Journal of Science: Mathematics - Physics

Journal homepage: https://js.vnu.edu.vn/MaP

Original Article

# The Nernst Effect in Infinite Semi-parabolic Asymmetric Quantum Wells with Electron-aacoustic Phonon Scattering in the Presence of Electromagnetic Wave

Nguyen Thu Huong[1], Nguyen Quang Son[1,*], Nguyen Dinh Nam[2]

[1]*Air Defence-Air Force Academy, Doai Phuong, Hanoi, Vietnam*

[2]*VNU University of Science, 334 Nguyen Trai, Thanh Xuan, Hanoi, Vietnam*

Received 22nd November 2025

Revised 06th January 2026; Accepted 9th April 2026

**Abstract:** We theoretically investigate the thermomagnetic Nernst effect in an infinite semi-parabolic asymmetric quantum well under the influence of a high-frequency electromagnetic wave. By using the quantum kinetic equation method, we derive analytical expressions for the Nernst coefficient, taking into account the electron-acoustic phonon interaction as the primary scattering mechanism. Numerical results show that the Nernst coefficient exhibits distinct Shubnikov-de Haas oscillations due to Landau quantization. We analyze in detail the dependence of the Nernst coefficient on temperature, magnetic field, confinement frequency, and electromagnetic wave frequency. A key finding is the contrasting influence of thermal and electromagnetic parameters: while increasing temperature significantly suppresses the oscillation amplitude via thermal broadening without affecting the peak positions, the presence of a high-frequency electromagnetic wave not only dampens the amplitude but also induces a shift in the resonance peaks. Additionally, the Nernst coefficient is found to be enhanced by a stronger confinement potential. These results suggest that the thermomagnetic properties of an infinite semi-parabolic asymmetric quantum well can be effectively tuned by external fields, offering potential applications in low-temperature nanodevices.

*Keywords:* Nernst effect, infinite semi-parabolic asymmetric quantum well, intense electromagnetic wave, quantum kinetic equation, electron–acoustic phonon scattering, Shubnikov-de Hass oscillation.

* Corresponding author.
*E-mail address:* sonnq@hus.edu.vn

https//doi.org/10.25073/2588-1124/vnumap.5096

## 1. Introduction

Low-dimensional semiconductor systems, particularly the infinite semi-parabolic asymmetric quantum well, have become focal points for thermoelectric research due to their tunable density of states [1-5]. While longitudinal transport is well-documented, the Nernst effect-a transverse thermomagnetic phenomenon—offers a far more sensitive probe of scattering dynamics and Fermi surface topology [6, 7].

The transport properties of such systems are profoundly altered by Landau quantization under a magnetic field and can be further manipulated by high-frequency electromagnetic waves [8]. Despite this, a theoretical treatment of the Nernst effect in the infinite semi-parabolic asymmetric quantum well under electromagnetic wave irradiation, specifically governed by the dominant low-temperature electron-acoustic phonon scattering mechanism [5], remains unexplored.

In this paper, we employ the quantum kinetic equation method to derive analytical expressions for the electric and thermal conductivity tensors, from which the Nernst coefficient is determined. We systematically investigate how the Nernst coefficient is modulated by the magnetic field, temperature, confinement potential, and electromagnetic wave frequency. The paper is organized as follows: Section 2 presents the transport equation for electrons; Section 3 derives the analytical expressions for the kinetic tensors and the Nernst coefficient; Section 4 presents the numerical results and discussion; and Section 5 provides the conclusion.

## 2. Transport Equation for Electrons

In this work, we investigate the transport properties of an electron gas in an asymmetric semi-parabolic quantum well. The electrons are confined in the z-direction by an infinite semi-parabolic potential part ($m_e\omega_z^2 z^2/2$) with the characteristic frequency ($\omega_z$), while they remain free to move in the x-y plane. A uniform magnetic field $\mathbf{B} \parallel z$ is applied perpendicular to the well, and a dc electric field $\mathbf{E} \parallel x$ drives the in-plane electron motion. Within the Landau gauge for the vector potential $\mathbf{A} = (0, Bx, 0)$, the single-particle Hamiltonian ($H_0$), together with its normalized eigenfunctions $|\xi\rangle$ and their eigenvalues ($\mathcal{E}_\xi$) corresponding to the semi-parabolic confinement, can be formulated as follows [9, 10]:

$$H_0 = -\frac{(\mathbf{p} + e\mathbf{A})^2}{2m_e} + \frac{m_e\omega_z^2 z^2}{2} + eEx\,, \tag{1}$$

$$|N, n, k_y\rangle = \frac{e^{ik_y y}}{\sqrt{L_y}}\,\phi_N(x - x_0)\phi_n(z)\,, \tag{2}$$

$$\mathcal{E}_{n,N}(\mathbf{k}_y) = \mathcal{E}_n + \hbar\omega_c\left(N + \frac{1}{2}\right) + \hbar v_d k_y - \frac{1}{2}m_e v_d^2\,; N = 0,1,2,\dots\,, \tag{3}$$

Here, e denotes the elementary charge of the electron, and $\mathbf{p}$ is the canonical momentum operator. The electron effective mass is taken to be $m_e = 0.067m_0$, with $m_0$ being the free electron rest mass. The functions $\phi_N(x - x_0)$ correspond to the standard harmonic-oscillator eigenstates, whose centers are shifted by $x_0 = (m_e v_d \ell_c^2)/\hbar - \ell_c^2 k_y$ , where $\mathbf{k}_y$ is the wave vector along the y-axis and $L_y$ represents the normalization length in that direction. The characteristic magnetic length is defined as $\ell_c = \sqrt{\hbar/(m_e\omega_c)}$, with the cyclotron frequency given by $\omega_c = eB/m_e$. The drift motion induced by the in-plane electric field is characterized by the velocity $v_d = E/B$. In the notation used, n labels the subband index associated with the confinement potential, whereas N stands for the Landau level quantum number. For an infinite semi-parabolic asymmetric quantum well, the one-electron normalized

eigenfunctions in the conduction band, together with their associated energy eigenvalues, can be expressed in the following form:

$$\phi_n(z) = |n\rangle = \sqrt{\frac{2n!}{\ell_z^3 \Gamma\left(n+\frac{3}{2}\right)}} e^{\left(-\frac{z^2}{2\ell_z^2}\right)} z L_n^{\frac{1}{2}}\left(\frac{z^2}{\ell_z^2}\right), \tag{4}$$

$$\mathcal{E}_n = \hbar\omega_z\left(2n+\frac{3}{2}\right); \quad n = 0,1,2,\ldots, \tag{5}$$

where $\Gamma(x)$ is the Gamma function, $L_n^k(x)$ is the associated Laguerre polynomial, and $\ell_z = \sqrt{\hbar/(m_e\omega_z)}$ is the characteristic confinement.

When the system is subjected to a strong electromagnetic wave whose electric field takes the form $\mathbf{E}(t) = (0, E_0 \sin\Omega t, 0)$ with $E_0$ and $\Omega$ being the field amplitude and angular frequency, respectively, the interaction can be incorporated through the corresponding vector potential

$\mathbf{A}(t) = (0, (E_0 \cos(\Omega t))/\Omega, 0)$, the Hamiltonian of the electron-phonon system, in the second quantization representation, can be written similarly to the ones obtained in Ref. [1]. Then, one can obtain an equation for the time-dependent electron distribution function as

$$\begin{aligned}
&\frac{\partial f_{N,n,\mathbf{k}_y}}{\partial t} + \left(\mathbf{F} + \omega_c[\mathbf{k}_y, \mathbf{h}]\right)\frac{\partial f_{N,n,\mathbf{k}_y}}{\hbar\,\partial \mathbf{k}_y} = \\
&= -\frac{2\pi}{\hbar}\sum_{N,n,N',n',\mathbf{q}} \left|\mathcal{C}_{\mathbf{q}}^{AP}\Im_{n,n'}(q_z)\mathcal{J}_{N,N'}(q_\perp)\right|^2 \sum_{s=-\infty}^{+\infty} J_s^2\left(\lambda q_y\right)(2N_q+1) \\
&\times\left\{\left[f_{N',n',\mathbf{k}_y+\mathbf{q}_y}(N_q+1) - f_{N,n,\mathbf{k}_y}N_q\right]\delta\left(\mathcal{E}_{n',N'}(\mathbf{k}_y+\mathbf{q}_y) - \mathcal{E}_{n,N}(\mathbf{k}_y) - s\hbar\Omega\right)\right. \\
&\left.+\left[f_{N',n',\mathbf{k}_y-\mathbf{q}_y}N_q - f_{N,n,\mathbf{k}_y}(N_q+1)\right]\delta\left(\mathcal{E}_{n',N'}(\mathbf{k}_y-\mathbf{q}_y) - \mathcal{E}_{n,N}(\mathbf{k}_y) - s\hbar\Omega\right)\right\},
\end{aligned} \tag{6}$$

In this formulation, the scattering between electrons and acoustic phonons is treated as an elastic process, allowing the acoustic phonon energy to be neglected [11]. The generalized force acting on electrons is given by $\mathbf{F} = e\mathbf{E} + \frac{\mathcal{E}-\mathcal{E}_F}{T}\nabla T$, where $\mathcal{E}$ and $\mathcal{E}_F$ denote the electron and Fermi energies, respectively. The unit vector along the magnetic-field direction is represented by $\mathbf{h} = \mathbf{B}/B$, and $\hbar$ is the reduced Planck constant. The quantity $J_s(x)$ stands for the Bessel function of order $s$ with argument x, while $\lambda = (eE_0)/(m_e\Omega^2)$ characterizes the dressing effect induced by the electromagnetic wave on the electronic states. The symbol $\delta(x)$ denotes the Dirac delta function, and $N_q$ is the equilibrium phonon occupation number following the Bose–Einstein distribution. The phonon wave vector is written as $\mathbf{q} = (\mathbf{q}_\perp, \mathbf{q}_z)$, where $\mathbf{q}_z$ is the out-of-plane component along the confinement direction and $\mathbf{q}_\perp$discribes the in-plane component. The coefficient $\mathcal{C}_{\mathbf{q}}^{AP}$ donates the electron–acoustic phonon coupling constant.

$$\left|\mathcal{C}_{\mathbf{q}}^{AP}\right|^2 = \frac{\hbar\mathcal{D}^2 q}{2\rho v_s V_0}, \tag{7}$$

here, $V_0 = L_x L_y L$ denotes the normalization volume of the quantum well structure, while $\mathcal{D}$, $\rho$, and $v_s$ represent the acoustic deformation potential, the mass density of the crystal, and the sound velocity, respectively. The quantities $\Im_{n,n'}(q_z)$ and $\mathcal{J}_{N,N'}(q_\perp)$ correspond to the electron and magnetic form factors in an infinite semi-parabolic asymmetric quantum well, and they are defined by

$$\Im_{n,n'}(q_z) = \langle n\left|e^{\pm iq_z z}\right|n'\rangle, \tag{8}$$

$$|\mathcal{J}_{N,N'}(q_\perp)|^2 = \left|\langle\phi_N(x-x_0)\left|e^{\pm iq_x x}\right|\phi_{N'}(x-x_0)\rangle\right|^2$$

$$= \frac{\mathrm{N}!\,\mathrm{e}^{-\alpha}}{\mathrm{N}'!}(\alpha)^{\mathrm{N}'-\mathrm{N}}\mathrm{L}_{\mathrm{N}}^{\mathrm{N}'-\mathrm{N}}(\alpha), \tag{9}$$

where, $\alpha = (\mathrm{q}_{\perp}^2\ \ell_{\mathrm{c}}^2)/2$.

## 3. Analytical Expression for the Kinetic Tensors and the Nernst Coefficient

By multiplying both sides of Eq. (6) by $\frac{\mathrm{e}\hbar}{\mathrm{m_e}}\mathbf{k}_{\mathrm{y}}\delta\left(\mathcal{E}-\mathcal{E}_{\mathrm{n,N}}(\mathbf{k}_{\mathrm{y}})\right)$ and subsequently summing over all subband indices n, Landau levels N, and wave vectors $\mathbf{k}_{\mathrm{y}}$, one arrives at a more compact expression for the kinetic equation. To simplify the treatment, the analysis is limited to single-photon absorption and emission processes, which effectively restricts the Bessel-function contributions in Eq. (6) to the orders $s = 0, \pm 1$. With these assumptions and after straightforward algebraic rearrangements, Eq. (6) can be transformed into the following form:

$$\frac{\mathfrak{R}(\mathcal{E})}{\tau(\mathcal{E})} + \omega_{\mathrm{c}}[\mathbf{h}, \mathfrak{R}(\mathcal{E})] = \boldsymbol{\mathcal{X}}(\mathcal{E}) + \boldsymbol{\mathcal{Y}}(\mathcal{E})\,, \tag{10}$$

$$\boldsymbol{\mathcal{X}}(\mathcal{E}) = -\frac{\mathrm{e}\hbar}{\mathrm{m_e}}\sum_{\mathrm{N,n,}\mathbf{k}_{\mathrm{y}}}\mathbf{k}_{\mathrm{y}}\left(\mathbf{F}, \frac{\partial \mathrm{f}_{\mathrm{N,n,}\mathbf{k}_{\mathrm{y}}}}{\partial \mathbf{k}_{\mathrm{y}}}\right)\delta\left(\mathcal{E}-\mathcal{E}_{\mathrm{n,N}}(\mathbf{k}_{\mathrm{y}})\right), \tag{11}$$

$$\begin{aligned}
\boldsymbol{\mathcal{Y}}(\mathcal{E}) \;=\; & \frac{2\pi\mathrm{e}}{\mathrm{m_e}}\sum_{\mathrm{N',n'}}\sum_{\mathrm{N,n}}\sum_{\mathbf{k}_{\mathrm{y}},\mathbf{q}}\left|\mathcal{M}_{\mathrm{n,n',N,N'}}(\mathrm{q})\right|^2 \mathrm{N_q}\mathbf{k}_{\mathrm{y}}\delta\left(\mathcal{E}-\mathcal{E}_{\mathrm{n,N}}(\mathbf{k}_{\mathrm{y}})\right)\times \\
& \times\left\{\left(\mathrm{f}_{\mathrm{N',n',}\mathbf{k}_{\mathrm{y}}+\mathbf{q}}-\mathrm{f}_{\mathrm{N',n',}\mathbf{k}_{\mathrm{y}}}\right)\left[\left(1-\frac{\mathfrak{Z}^2\mathbf{q}_y^2}{2}\right)\delta\left(\mathcal{E}_{\mathrm{n',N'}}(\mathbf{k}_{\mathrm{y}}+\mathbf{q}_{\mathrm{y}})-\mathcal{E}_{\mathrm{n,N}}(\mathbf{k}_{\mathrm{y}})\right)+\right.\right. \\
& \left.\left.+\frac{\mathfrak{Z}^2\mathbf{q}_y^2}{4}\delta\left(\mathcal{E}_{\mathrm{n',N'}}(\mathbf{k}_{\mathrm{y}}+\mathbf{q}_{\mathrm{y}})-\mathcal{E}_{\mathrm{n,N}}(\mathbf{k}_{\mathrm{y}})\pm\hbar\Omega\right)\right]+ \\
& \left\{\left(\mathrm{f}_{\mathrm{N',n',}\mathbf{k}_{\mathrm{y}}-\mathbf{q}}-\mathrm{f}_{\mathrm{N',n',}\mathbf{k}_{\mathrm{y}}}\right)\left[\left(1-\frac{\mathfrak{Z}^2\mathbf{q}_y^2}{2}\right)\delta\left(\mathcal{E}_{\mathrm{n',N'}}(\mathbf{k}_{\mathrm{y}}-\mathbf{q}_{\mathrm{y}})-\mathcal{E}_{\mathrm{n,N}}(\mathbf{k}_{\mathrm{y}})\right)+\right.\right. \\
& \left.\left.\left.+\frac{\mathfrak{Z}^2\mathbf{q}_y^2}{4}\delta\left(\mathcal{E}_{\mathrm{n',N'}}(\mathbf{k}_{\mathrm{y}}-\mathbf{q}_{\mathrm{y}})-\mathcal{E}_{\mathrm{n,N}}(\mathbf{k}_{\mathrm{y}})\pm\hbar\Omega\right)\right]\right\}\,,
\end{aligned} \tag{12}$$

In this expression, $\tau(\mathcal{E})$ denotes the energy-dependent relaxation time of the carriers, while $\mathfrak{R}(\mathcal{E})$ characterizes the partial contribution to the current density arising from electrons with energy $\mathcal{E}$.

By solving Eq. (6), one arrives at the following expression:

$$\begin{aligned}
\mathfrak{R}(\mathcal{E}) \;=\; & \frac{\tau(\varepsilon)}{1+\omega_{\mathrm{c}}^2\tau^2(\varepsilon)}\{\boldsymbol{\mathcal{X}}(\mathcal{E})+\boldsymbol{\mathcal{Y}}(\mathcal{E})-\omega_{\mathrm{c}}\tau(\varepsilon)[\boldsymbol{\mathcal{X}}(\mathcal{E})+\boldsymbol{\mathcal{Y}}(\mathcal{E})]+ \\
& +\omega_{\mathrm{c}}^2\tau^2(\varepsilon)\mathbf{h}\left(\mathbf{h}, \boldsymbol{\mathcal{X}}(\mathcal{E})+\boldsymbol{\mathcal{Y}}(\mathcal{E})\right)\}
\end{aligned} \tag{13}$$

The total current density is determined by

$$\mathbf{j}(\mathrm{t}) = \int_0^{+\infty}\mathfrak{R}(\mathcal{E})\mathrm{d}\mathcal{E} = \frac{\mathrm{e}\hbar}{\mathrm{m_e}}\int_0^{+\infty}\sum_{\mathrm{N,n,}\mathbf{k}_{\mathrm{y}}}\mathbf{k}_{\mathrm{y}}\,\mathrm{f}_{\mathrm{N,n,}\mathbf{k}_{\mathrm{y}}}(\mathrm{t})\delta\left(\mathcal{E}-\mathcal{E}_{\mathrm{n,N}}(\mathbf{k}_{\mathrm{y}})\right)\mathrm{d}\mathcal{E}\,. \tag{14}$$

From the obtained expression for the total current density **j,** one can determine the electrical conductivity tensor $\sigma_{\mathrm{im}}^{\mathrm{AP}}$ and the thermoelectric tensor $\beta_{\mathrm{im}}^{\mathrm{AP}}$ by employing the standard the thermoelectric transport relation [12],

$$\mathbf{j} = \sigma_{\mathrm{im}}^{\mathrm{AP}}\mathbf{E}_{\mathrm{m}} + \beta_{\mathrm{im}}^{\mathrm{AP}}\boldsymbol{\nabla}\mathbf{T}_{\mathrm{m}}\,. \tag{15}$$

Based on the equations (14) and (15), we can obtain the expression of the tensors:

$$\sigma_{xx}^{AP} = \frac{\tau(\mathcal{E}_F)(1-\omega_c\tau)}{1+\omega_c^2\tau^2(\mathcal{E}_F)}\wp_0^{AP} + \left(\mathcal{K}_1^{AP}+\mathcal{K}_2^{AP}\right)\wp_1^{AP} + \mathcal{K}_3^{AP}\wp_2^{AP} + \mathcal{K}_4^{AP}\wp_3^{AP} \quad (21)$$

$$\begin{aligned}\sigma_{xy}^{AP} &= \frac{\tau(\mathcal{E}_F)(1-\omega_c\tau)}{1+\omega_c^2\tau^2(\mathcal{E}_F)}\wp_0^{AP} + \left(\mathcal{K}_1^{AP}+\mathcal{K}_2^{AP}\right)\wp_1^{AP}\omega_c^2\tau^2(\Delta_\mathcal{E}) + \\ &+\mathcal{K}_3^{AP}\wp_2^{AP}\omega_c^2\tau^2(\Delta_\mathcal{E}-\hbar\Omega) + \mathcal{K}_4^{AP}\wp_3^{AP}\omega_c^2\tau^2(\Delta_\mathcal{E}+\hbar\Omega)\end{aligned} \quad (22)$$

$$\begin{aligned}\beta_{xx}^{AP} &= -\left(\mathcal{K}_1^{AP}+\mathcal{K}_2^{AP}\right)\frac{(\Delta_\mathcal{E}-\varepsilon_F)\wp_1^{AP}}{T} - \mathcal{K}_3^{AP}\frac{(\Delta_\mathcal{E}-\hbar\Omega-\varepsilon_F)\wp_2^{AP}}{T} - \\ &-\mathcal{K}_4^{AP}\frac{(\Delta_\mathcal{E}+\hbar\Omega-\varepsilon_F)\wp_3^{AP}}{T},\end{aligned} \quad (23)$$

$$\begin{aligned}\beta_{xy}^{AP} &= -\left(\mathcal{K}_1^{AP}+\mathcal{K}_2^{AP}\right)\frac{(\Delta_\mathcal{E}-\varepsilon_F)\wp_1^{AP}\omega_c^2\tau^2(\Delta_\mathcal{E})}{T} - \\ &-\mathcal{K}_3^{AP}\frac{(\Delta_\mathcal{E}-\hbar\Omega-\varepsilon_F)\wp_2^{AP}\omega_c^2\tau^2(\Delta_\mathcal{E}-\hbar\Omega)}{T} - \\ &-\mathcal{K}_4^{AP}\frac{(\Delta_\mathcal{E}+\hbar\Omega-\varepsilon_F)\wp_3^{AP}\omega_c^2\tau^2(\Delta_\mathcal{E}+\hbar\Omega)}{T},\end{aligned} \quad (24)$$

where,

$$\wp_0^{AP} = \frac{eL_y}{2\pi m_e\hbar^2 v_d}\mathcal{E}_{n,N}(\mathbf{k}_y); \qquad \Delta_\mathcal{E} = \mathcal{E}_{n',N'} - \mathcal{E}_{n,N} + eE_1\lambda.$$

$$\wp_1^{AP} = \frac{e\,\tau^2(\Delta_\mathcal{E})}{m_e[1+\omega_c^2\tau^2(\Delta_\mathcal{E})]^2}; \qquad \wp_2^{AP} = \frac{e\,\tau^2(\Delta_\mathcal{E}-\hbar\Omega)}{m_e[1+\omega_c^2\tau^2(\Delta_\mathcal{E}-\hbar\Omega)]^2}$$

$$\wp_3^{AP} = \frac{e\,\tau^2(\Delta_\mathcal{E}+\hbar\Omega)}{m_e[1+\omega_c^2\tau^2(\Delta_\mathcal{E}+\hbar\Omega)]^2}; \quad \lambda = \left(\sqrt{N+\frac{1}{2}}+\sqrt{N+\frac{3}{2}}\right)\frac{\ell_c}{2};$$

$$\mathcal{E}_{n,N}(\mathbf{k}_y) = \hbar\omega_z\left(2n+\frac{3}{2}\right) + \hbar\omega_c\left(N+\frac{1}{2}\right) + \hbar v_d k_y - \frac{1}{2}m_e v_d^2;$$

$$\mathcal{E}_{n',N'} = \hbar\omega_z\left(2n'+\frac{3}{2}\right) + \hbar\omega_c\left(N'+\frac{1}{2}\right) - \frac{1}{2}m_e v_d^2$$

$$\mathcal{E}_{n,N} = \hbar\omega_z\left(2n+\frac{3}{2}\right) + \hbar\omega_c\left(N+\frac{1}{2}\right) - \frac{1}{2}m_e v_d^2$$

$$\mathcal{K}_1^{AP} = \mathfrak{S}\left(1-\frac{\mathfrak{Z}^2\lambda^2}{2\ell_c^2}\right)\left[1+2\sum_{l=1}^{\infty}(-1)^l e^{\left(-\frac{2\pi l\alpha}{\hbar\omega_c}\right)}\cos(2\pi l\bar{\varkappa}_1)\right]$$

$$\mathcal{K}_2^{AP} = \mathfrak{S}\frac{\mathfrak{Z}^2\lambda^2}{4\ell_c^2}\left[1+2\sum_{l=1}^{\infty}(-1)^l e^{\left(-\frac{2\pi l\alpha}{\hbar\omega_c}\right)}\cos(2\pi l\bar{\varkappa}_1)\right]$$

$$\mathcal{K}_3^{AP} = \mathfrak{S}\frac{\mathfrak{Z}^2\lambda^2}{4\ell_c^2}\left[1+2\sum_{l=1}^{\infty}(-1)^l e^{\left(-\frac{2\pi l\alpha}{\hbar\omega_c}\right)}\cos(2\pi l\bar{\varkappa}_2)\right]$$

$$\mathcal{K}_4^{AP} = \mathfrak{S}\frac{\mathfrak{Z}^2\lambda^2}{4\ell_c^2}\left[1+2\sum_{l=1}^{\infty}(-1)^l e^{\left(-\frac{2\pi l\alpha}{\hbar\omega_c}\right)}\cos(2\pi l\bar{\varkappa}_3)\right]$$

$$\overline{\varkappa}_1 = \frac{\mathcal{E}_{n,N} - \mathcal{E}_{n',N'} + eE_1\lambda}{\hbar\omega_c}; \quad \overline{\varkappa}_2 = \overline{\varkappa}_1 - \frac{\Omega}{\omega_c}$$

$$\overline{\varkappa}_3 = \overline{\varkappa}_1 + \frac{\Omega}{\omega_c}; \quad \alpha = \frac{\hbar}{\tau};$$

$$\mathfrak{S} = \frac{e\eta_0\mathcal{D}^2 m_e k_B T L_y L}{8\pi^2\hbar^4\rho v_d v_s^3}\int_{-\infty}^{+\infty}\left|\Im_{n,n'}(q_z)\right|^2\lambda(\mathcal{E}_{n,N} - \varepsilon_F)\,dq_z\,,$$

with $\eta_0$ being the electron's density. The Nernst coefficient can be determined from the conductivity and thermoelectric tensors (given in Eqs. (21–24)) using the following relation

$$NC = -\frac{1}{B}\frac{\sigma_{xx}^{AP}\cdot\beta_{xy}^{AP} - \sigma_{xy}^{AP}\cdot\beta_{xx}^{AP}}{(\sigma_{xx}^{AP})^2 + \left(\sigma_{xy}^{AP}\right)^2} \tag{25}$$

## 4. Numerical Results and Discussion

To elucidate the physical significance of the obtained analytical expressions, the Nernst coefficient (NC) is numerically evaluated for GaAs/AlGaAs heterostructures using typical material parameters [13, 14]: $\mathcal{E}_F = 50$ meV, $m_e = 0.067\ m_o$ (where $m_0 = 9.1\times10^{-31}$ kg, which is the mass of a free electron), $\tau = 10^{-12}$ s, $v_s = 5220$ m/s, $e_0 = 1.6\times10^{-19}$ C, e = 2.07$e_0$, and $\mathcal{E}_0 = 8.86\times10^{-12}\ C^2m^{-2}N^{-1}$. The frequencies are selected to investigate the high-frequency regime ($\Omega\sim10^{13}$ Hz) and to ensure that the confinement energy is comparable to the cyclotron energy($\omega_z\sim10^{12}$ Hz). In the present calculation, only transitions between the nearest energy levels are considered, whereas contributions from higher-state transitions are neglected.

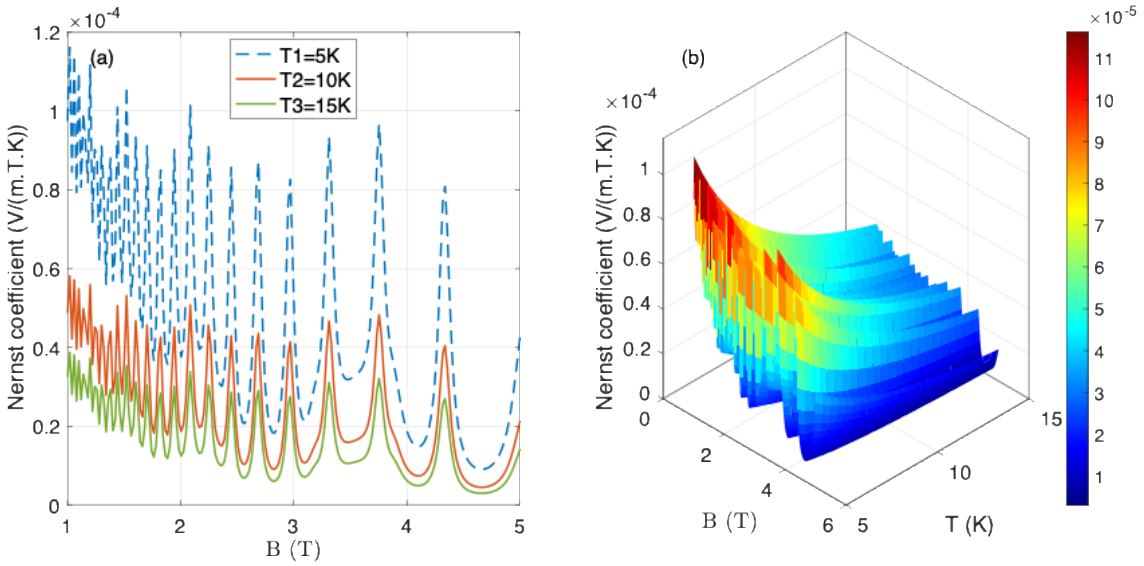


Figure 1. (a) The dependence of the Nernst coefficient on the magnetic field B for three different values of temperature T. (b) The dependence of the Nernst coefficient on the magnetic field B and temperature T.

Figure 1(a) illustrates the magnetic field dependence of the Nernst coefficient within the range of 1 T to 5 T at three representative temperatures: T1=5K (dark blue dashed curve), T2=10K (burnt orange

curve), and T3=15K (olive green curve). A salient feature of the data is the emergence of pronounced quantum oscillations with significant amplitudes, reflecting the discrete nature of Landau levels passing through the Fermi surface. The period of these oscillations expands with increasing magnetic field, adhering to the characteristic 1/B periodicity. In terms of amplitude, the Nernst coefficient demonstrates high sensitivity to temperature; the signal peaks at T=5 K and is markedly suppressed as the temperature rises to 10 K and 15 K. This amplitude reduction serves as empirical evidence for the thermal broadening effect, where the widening of the Fermi-Dirac distribution at higher temperatures smears out the van Hove singularities in the density of states [15]. Crucially, it is observed that the positions of the oscillatory peaks remain invariant as the temperature increases from 5 K to 15 K. This phase stability confirms that the Landau level structure, determined by the magnetic field B, remains robust and is not altered by temperature within the investigated range. Temperature acts solely to suppress the amplitude via thermal broadening of the Fermi distribution, without shifting the quantum resonance conditions [4, 12].

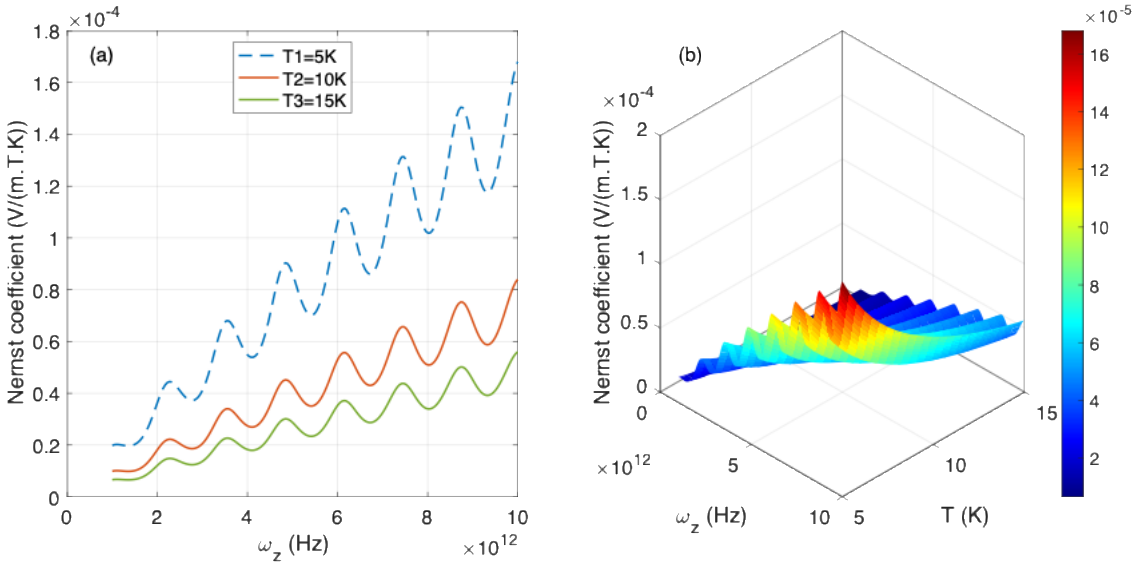


Figure 2. (a) The dependence of the Nernst coefficient on the confinement frequency $\omega_z$ for three different values of temperature T. (b) The dependence of the Nernst coefficient on confinement frequency $\omega_z$ and temperature T.

To provide a more comprehensive perspective on the carrier dynamics, Figure 1(b) displays the Nernst coefficient as a 3D surface plot as a function of both magnetic field and temperature. The topological surface highlights the transition from a regime of strong oscillations at low temperatures to a damped state at higher temperatures. The sharp oscillatory peaks observed in the vicinity of T=5K rapidly flatten as one moves along the temperature axis toward 15K, resulting in a smoother surface with reduced Nernst coefficient values. This damping of the Shubnikov-de Haas-type oscillations confirms that as the thermal energy $k_BT$ becomes comparable to the cyclotron energy spacing $\hbar\omega_c$, macroscopic quantum effects are increasingly overshadowed by thermal scattering, leading to a suppression of the thermomagnetic response.

Figure 2(a) depicts the variation of the Nernst coefficient as a function of the confinement frequency $\omega_z$ in the range of $1 \times 10^{12}$ Hz to $10 \times 10^{12}$ Hz. Unlike the magnetic field dependence, the Nernst signal here exhibits a monotonic increase in magnitude with increasing $\omega_z$ , suggesting that stronger confinement enhances the thermomagnetic response. Superimposed on this rising baseline are distinct

quantum oscillations, which arise from the crossing of quantization subbands—induced by the confinement potential—through the Fermi energy. The amplitude of these oscillations is strongly temperature-dependent: at T=5K, the peaks are sharp and pronounced. However, as the temperature rises to 10 K and 15 K, the oscillation amplitude is significantly suppressed, and the peaks become broadened. This behavior reflects the interplay between the quantization energy $\hbar\omega_z$ and the thermal energy $k_BT$; at higher temperatures, thermal broadening smears out the discrete structure of the density of states, leading to the damping of the oscillatory features. Similar to the magnetic field dependence, the positions of the resonant peaks along the $\omega_z$-axis are preserved across all investigated temperatures. This indicates that the spacing between the subbands is an intrinsic property of the confinement potential and is independent of T. The amplitude suppression is purely a consequence of the discrete quantum states being smeared out by the thermal energy.

Figure 2(b) provides a comprehensive visualization of the Nernst coefficient's dependence on both $\omega_z$ and T. The surface plot reveals that the coefficient reaches its maximum values in the regime of high confinement frequency and low temperature (dark red region). A clear transition is observable: in the low-temperature region (T<10K), 'ripples' corresponding to quantum oscillations are clearly defined along the $\omega_z$-axis. Conversely, moving towards the higher temperature region (T>10K), the surface becomes smoother, and the increasing trend with respect to $\omega_z$ becomes continuous without sharp discontinuities. This damping of oscillations in the 3D model reaffirms the dominant role of thermal scattering in suppressing quantum size effects within the investigated temperature range.

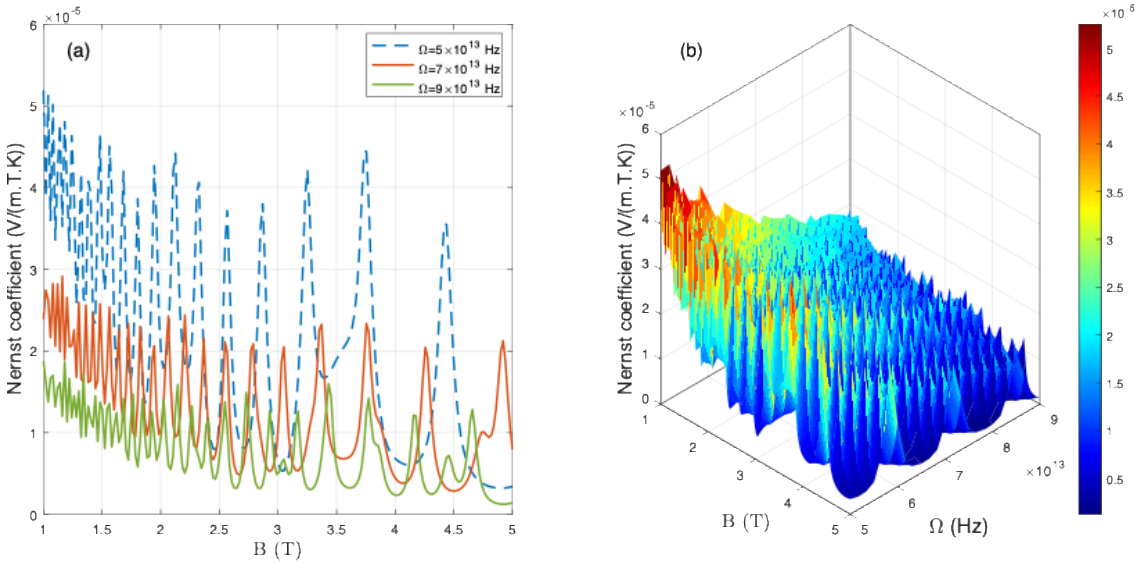


Figure 3. (a) The dependence of the Nernst coefficient on the magnetic field B for three different values of the intense electromagnetic wave frequency Ω. (b) The dependence of the Nernst coefficient on the magnetic field B and intense electromagnetic wave frequency Ω.

Figure 3(a) describes the magnetic field dependence of the Nernst coefficient under electromagnetic wave irradiation at three distinct frequencies: $\Omega = 5 \times 10^{13}$ Hz, $\Omega = 7 \times 10^{13}$ Hz, and $\Omega = 10 \times 10^{13}$ Hz. Quantum oscillations periodic in 1/B remain clearly visible, indicating that the Landau level structure is preserved under the external field. However, an intriguing 'quenching' effect is observed: the

oscillation amplitude is maximized at the lowest frequency ($\Omega = 5 \times 10^{13}$ Hz, dark blue dashed curve) and undergoes substantial suppression as the frequency increases. At $\Omega = 9 \times 10^{13}$ Hz (olive green curve), the oscillatory peaks are markedly dampened. This suggests that high photon energy ($\hbar\Omega$) may interfere with scattering processes or renormalize band parameters (such as the effective mass), thereby inhibiting the thermomagnetic response of the system. In stark contrast to the temperature effect, varying the electromagnetic wave frequency $\Omega$ results in a distinct shift in the positions of the oscillatory peaks. This peak shifting phenomenon suggests that the external field frequency $\Omega$ directly modifies the electron energy spectrum, thereby altering the specific Landau resonance conditions. Similar peak-shifting phenomena induced by intense electromagnetic fields have been reported in semi-parabolic quantum wells [10] and are supported by the theory of microwave-irradiated transport [7].

The comprehensive landscape of the electromagnetic field's influence is depicted in the 3D plot in Figure 3(b), which maps the Nernst coefficient as a function of both magnetic field B and frequency $\Omega$. The topological surface reveals that the oscillatory peaks are prominent in the low-frequency regime and are progressively eroded as one traverses the $\Omega$-axis towards higher values. This transition from a high-amplitude oscillatory regime to a suppressed state occurs uniformly across the investigated magnetic field range. These results indicate that, in addition to temperature, the frequency of the external field serves as an effective control parameter for tuning the magnitude of the Nernst effect; specifically, increasing the electromagnetic wave frequency tends to diminish macroscopic quantum transport properties within the material.

## 5. Conclusion

We have theoretically investigated the Nernst effect in an infinite semi-parabolic asymmetric quantum well under the influence of an electromagnetic wave and electron-acoustic phonon interaction. The numerical results indicate that the Nernst coefficient exhibits distinct Shubnikov-de Haas oscillations with a 1/B periodicity. Increasing temperature significantly suppresses the oscillation amplitude due to thermal broadening, yet the positions of the resonance peaks remain invariant. A stronger confinement frequency $\omega_z$ notably enhances the magnitude of the Nernst signal. In contrast, high-frequency electromagnetic radiation ($\Omega$) not only dampens the amplitude but also induces a shift in the peak positions. These findings demonstrate the tunability of the thermomagnetic properties of infinite semi-parabolic asymmetric quantum well via external fields, suggesting potential applications in low-temperature nanodevices.

## References

[1] C. T. V. Ba, N. Q. Bau, N. T. L. Quynh, N. D. Nam, D. T. Long, Theoretical Study of Photo-stimulated Thermo-magnetoelectric Effects in Two-Dimensional Compositional Superlattices Using Quantum Kinetic Equation, Journal of the Korean Physical Society, Vol. 81, No. 8, 2022, pp. 757-769, https://doi.org/10.1007/s40042-022-00584-x.

[2] Y. G. Gurevich, G. N. Logvinov, Physics of Thermoelectric Cooling, Semiconductor Science and Technology, Vol. 20, No. 12, 2005, pp. R57, https://doi.org/10.1088/0268-1242/20/12/R01.

[3] A. F. Ioffe, L. S. Stil'bans, E. K. Iordanishvili, T. S. Stavitskaya, A. Gelbtuch, Semiconductor Thermoelements and Thermoelectric Cooling, Physics Today, Vol. 12, No. 5, 1959, pp. 42, https://doi.org/10.1063/1.3060810.

[4] T. T. Dien, C. T. V. Ba, N. Q. Bau, N. T. N. Anh, Calculation of Parallel Peltier Coefficient in Rectangular Quantum Wires under the Influence of Confined Optical Phonons and Electromagnetic Waves Using Quantum Kinetic Equation, Journal of the Korean Physical Society, Vol. 82, 2023, pp. 1187-1195, https://doi.org/10.1007/s40042-023-00781-2.

[5] L. T. Hung, N. T. L. Quynh, N. T. N. Anh, N. Q. Bau, The Influence of Confined Acoustic Phonon on the Quantum Peltier Effect in Doped Semiconductor Superlattice in the Presence of Electromagnetic Wave, Journal of Physics: Conference Series, Vol. 1932, 2021, pp. 012009, https://doi.org/10.1088/1742-6596/1932/1/012009.

[6] N. Q. Bau, D. T. Hang, D. M. Quang, N. T. T. Nhan, Magneto–thermoelectric Effects in Quantum Well in the Presence of Electromagnetic Wave, VNU Journal of Science: Mathematics–Physics, Vol. 33, No. 2, 2017, pp. 1-9, https://doi.org/10.25073/2588-1124/vnumap.4071.

[7] O. E. Raichev, Theory of Magnetothermoelectric Phenomena in High-mobility Two-dimensional Electron Systems Under Microwave irradiation, Phys. Rev. B, Vol. 91, 2015, pp. 235307.

[8] K. Behnia, The Nernst effect and the Boundaries of the Fermi Liquid Picture, J. Phys. Condens. Matter, Vol. 21, 2009, pp. 113101.

[9] P. Vasilopoulos, M. Charbonneau, C. M. V. Vliet, Linear and Nonlinear Electrical Conduction in Quasi-Two-Dimensional Quantum Wells, Physical Review B, Vol. 35, No. 3, 1987, pp. 1334, doi.org/10.1103/PhysRevB.35.1334.

[10] N. T. Huong, N. Q. Bau, C. T. V. Ba and B. T. Dung, N. C. Toan, A. T. Tran, Theoretical Study of Magnetoresistance Oscillations in Semi-Parabolic Plus Semi-inverse Squared Quantum Wells in the Presence of Intense Electromagnetic Waves, Phys. Scr., Vol. 100, 2024, pp. 015984.

[11] P. Vasilopoulos, Magnetophonon Oscillations in Quasi-Two-Dimensional Quantum Wells, Physical Review B, Vol. 33, 1986, pp. 8587.

[12] N. Q. Bau, D. T. Hang, D. T. Long, Study of the Quantum Magneto-thermoelectric Effect in the Two-Dimensional Compositional Superlattice GaAs/AlGaAs under the Influence of an Electromagnetic Wave by Using the Quantum Kinetic Equation, J. Korean Phys. Soc., Vol. 75, 2019, pp. 1004-1016.

[13] B. K. Ridley, Quantum Processes in Semiconductors, Pub. Clarendon Press, Add. Oxford, 1993.

[14] J. Singh, Physics of Semiconductors and Their Heterostructures, Pub. McGraw-Hill, Add. Singapore, 1993.

[15] Y. Quan, W. E. Pickett, Van Hove Singularities and Spectral Smearing in High-temperature Superconducting $H_3S$, Phys. Rev. B, Vol. 93, pp. 104526, https://doi.org/10.1103/PhysRevB.93.104526.